phase environments (*20*) and, we may assume, were also abundant in the solar nebula. The alternative possibility exists that aliphatic hydrocarbons in the meteorite underwent condensation and aromatization as in terrestrial kerogens. However, such thermal alteration would not be consistent with the hydrogen abundance of the material, which implies an incomplete condensation of rings, the finding in the extracts of labile molecules, as nitriles, and the presence of a substantial aliphatic phase in more petrologically processed chondrites, as CVs (*7*).

Far from disappointing, the relative simplicity of Tagish Lake organic content provides insight into an outcome of early solar system chemical evolution not seen so far. In particular, the finding of just one suite of organic compounds matching those of Murchison and of some (but not all) the carbonaceous phases and compounds seen in other chondrites demonstrates the presence of distinct organic synthetic processes in primitive meteorites. It also implies that the more complex organic matter of heterogeneous chondrites may result from multiple, separate evolutionary pathways.

References and Notes

1. J. R. Cronin, S. Chang, in *The Chemistry of Life's Origins*, J. M. Greenberg, C. X. Mendoza-Gomez, V. Pirronello, Eds. (Kluwer Academic, Dordrecht, Netherlands, 1993), pp. 209–258, and references therein.
2. C. F. Chyba, C. Sagan, *Nature* **355**, 125 (1992).
3. P. G. Brown *et al.*, *Science* **290**, 320 (2000).
4. S. Pizzarello, G. W. Cooper, *Meteoritic Planet. Sci.* **36**, 897 (2001).
5. J. R. Cronin, S. Pizzarello, S. Epstein, R. V. Krishnamurthy, *Geochim. Cosmochim. Acta* **57**, 4745 (1993).
6. J. R. Cronin, S. Pizzarello, *Geochim. Cosmochim. Acta* **54**, 2859 (1990).
7. ———, J. S. Frye, *Geochim. Cosmochim. Acta* **51**, 299 (1987).
8. The compounds were analyzed by GC-MS as isopropyl esters. The GC columns were ChyrasilDEX (Chrompack; 25 m by 0.25 mm) or Chirasil-Val (Alltech; 50 m by 0.25 mm). The typical program was 40°C initial, 5 min; −100 at 2°/min; and −200 at 4°/min.
9. GC-C-IRMS: HP 6890 GC, Finnigan high-temperature conversion interphase III, and Mat Delta$^+$-XL MS. GC conditions were as for GC-MS (*8*). Oxidation was at 940°C with a ceramic oxidation reactor bearing NiO/CuO/Pt wires. Standard CO_2 (six pulses) $\delta^{13}C$: −10.07‰ (VPDB). Data were analyzed with Finnigan ISODAT software, with $\sigma < \pm 0.3$‰ for peaks >0.5 V.
10. −85‰ to −5‰, up to +5‰ for methanogenic bacteria.
11. These acids were analyzed with DB-17 column (60 m by 0.25 mm; Agilent Technologies). Other $\delta^{13}C$ values were +7.7 ± 0.3‰ for a methyl-phthalimide and +5.9 ± 0.7‰, +10.5 ± 0.8‰, and +17.5 ± 0.4‰ for three dimethyl-phthalimides.
12. J. G. Lawless, G. U. Yuen, *Nature* **282**, 396 (1979).
13. G. W. Cooper, M. H. Thiemens, T. Jackson, S. Chang, *Science* **277**, 1072 (1997), and references therein.
14. M. H. Studier, R. Hayatsu, E. Anders, *Geochim. Cosmochim. Acta* **36**, 189 (1972).
15. Airborne contamination can be absorbed readily by meteorites (*28*) and should be considered for Tagish Lake, which was recovered a week after its fall.
16. Operating conditions were as follows: Varian INOVA400 spectrometer at 9.4 T with the VACP MAS sequence, 50-kHz spectral width, 3.5-ms cross-polarization contact time, recycle delay of 1.04 s, 6.7-μs ^{1}H90 pulse width, 28,584 transients per spectrum, 55-kHz decoupling field, 16.0-kHz spinning rate, and 4-mm silicon nitride rotors with Torlon caps. Tagish Lake repeat analyses were at 0.5-, 1.0-, and 2.0-ms contact time.
17. G. D. Cody, C. M. O'D Alexander, F. Tera, *Lunar Planet. Sci.* **30** (abstract 1582) (1999) [CD-ROM].
18. A. Gardinier *et al.*, *Earth Planet. Sci. Lett.* **184**, 9 (2000).
19. δD values were determined by thermal conversion (TC)/elemental analyzer (EA) interfaced to Finnigan Delta$^+$XL MS. Pyrolysis was at 1450°C to yield hydrogen gas quantitatively. Standardization was by hydrogen gas pulse; sample analyses were repeated 10 times.
20. L. J. Allamandola, S. A. Sanford, B. Wopenka, *Science* **237**, 56 (1987).
21. J. F. Kerridge, S. Chang, R. Shipp, *Geochim. Cosmochim. Acta* **51**, 2527 (1987).
22. 1.3 ppm of fullerenes was isolated from the bulk carbonaceous residues by extraction with 1,2,3,5 tetramethylbenzene. The yield was incomplete, as for other meteorites (*23*), because of limited organic solubility of fullerenes.
23. L. Becker, R. J. Poreda, T. E. Bunch, *Proc. Natl. Acad. Sci. U.S.A.* **97**, 2979 (2000).
24. Helium within the extract was ~0.01% of total helium in the bulk material. About 40% of this total helium is released below 800°C, consistent with the extracted fullerene carrier. No other carbon carrier has been identified with similar low-temperature release pattern.
25. E. T. Peltzer, J. L. Bada, *Nature* **272**, 443 (1978).
26. I. Gilmour, M. A. Sephton, V. K. Pearson, *Lunar Planet. Sci.* **32** (abstract 1969) (2001).
27. I. Gilmour, V. K. Pearson, M. A. Sephton, *Lunar Planet. Sci.* **32** (abstract 1993) (2001).
28. J. Han, B. R. Simoneit, A. L. Burlingame, M. Calvin, *Nature* **222**, 364 (1969).
29. J. R. Cronin, S. Pizzarello, D. P. Cruikshank, in *Meteorites and the Early Solar System*, J. F. Kerridge, M. S. Matthews, Eds. (Univ. of Arizona Press, Tucson, AZ, 1988), pp. 819–8857.
30. G. W. Cooper, J. R. Cronin, *Geochim. Cosmochim. Acta* **59**, 1003 (1995).
31. $\delta‰ = (R_{sample} - R_{standard}/R_{standard}) \times 10^3$. For carbon, $R = {}^{13}C/{}^{12}C$ and the standard is VPDB. $\delta^{13}C$(VPDB) of isopropanol: −29.3‰ (EA-IRMS). $\delta^{13}C$ mass balance equations: $\delta^{13}C_{diacid} = [\delta^{13}C_{der.\ diacid} - a(-29.3)]/b$ (*a* and *b* are fractional carbon abundances of isopropanol and diacid, respectively). A procedural succinic acid standard gave no substantial carbon fractionation.

32. We thank M. Zolensky, A. Hildebrand, and J. Brook for providing the Tagish Lake sample; J. Cronin for much help and suggestions; C. Moore for supporting a student assistant; and four anonymous referees for helpful reviews. We gratefully acknowledge conversations with M. Bernstein, C. Chyba, J. Dworkin, I. Gilmour, D. Hudgins, W. Huebner, and A. Primak. The work was supported by NASA grants from the Exobiology (S.P., Y.H., and G.C.) and Cosmochemistry (L.B.) Divisions and NSF grant CHE9808678 (NMR).

17 May 2001; accepted 14 August 2001
Published online 23 August 2001;
10.1126/science.1062614
Include this information when citing this paper.

Origin of Whales from Early Artiodactyls: Hands and Feet of Eocene Protocetidae from Pakistan

Philip D. Gingerich,[1]* Munir ul Haq,[1,2] Iyad S. Zalmout,[1] Intizar Hussain Khan,[2,3] M. Sadiq Malkani[2]

Partial skeletons of two new fossil whales, *Artiocetus clavis* and *Rodhocetus balochistanensis*, are among the oldest known protocetid archaeocetes. These came from early Lutetian age (47 million years ago) strata in eastern Balochistan Province, Pakistan. Both have an astragalus and cuboid in the ankle with characteristics diagnostic of artiodactyls; *R. balochistanensis* has virtually complete fore- and hind limbs. The new skeletons are important in augmenting the diversity of early Protocetidae, clarifying that Cetacea evolved from early Artiodactyla rather than Mesonychia and showing how early protocetids swam.

Whales are marine mammals grouped in the order Cetacea (*1*). Most mammals live on land and the fossil record of early mammals is terrestrial. Thus, it has long been reasonable to infer that the origin of whales involved an evolutionary transition from land to sea. This is one of the most profound changes of adaptive zone amenable to study in the fossil record. Living whales are so distinctive, and intermediate fossils sufficiently rare, that a half-century ago Simpson regarded Cetacea as "on the whole the most peculiar and aberrant of mammals," inserting them arbitrarily in his classic 1945 classification of mammals (*2*). In response, Boyden and Gemeroy (*3*) applied innovative immunological precipitin tests and found much higher cross-reactivity of Cetacea to Artiodactyla than to other living orders of mammals. Van Valen (*4*) attempted to reconcile close relationship of whales and artiodactyls with the then-known fossil record by proposing that whales originated from Paleocene mesonychid condylarths,

[1]Department of Geological Sciences and Museum of Paleontology, The University of Michigan, Ann Arbor, MI 48109–1079, USA. [2]Geological Survey of Pakistan, Sariab Road, Quetta, Pakistan. [3]Department of Earth Sciences, University of New Hampshire, Durham, NH 03824–3589, USA.

*To whom correspondence should be addressed. E-mail: gingeric@umich.edu

whereas artiodactyls originated from closely related Paleocene arctocyonid condylarths. Most morphologists and paleontologists have favored a mesonychid origin of whales (*5*–*14*), but further immunological, DNA hybridization, and molecular sequencing studies support close relationship of Cetacea to artiodactyls (*15*–*18*) and more specifically to hippopotami within Artiodactyla (*19*–*27*). Here we provide paleontological evidence showing that whales evolved from early artiodactyls rather than mesonychid condylarths.

Artiodactyla (Greek *artios*, entire or even-numbered, and *dactylos*, finger or toe) are named for the even number (two or four) of manual and pedal digits (fingers and toes) found on each hand (manus) and foot (pes) in extant taxa. Ankle or tarsal bones are the most diagnostic elements of the artiodactyl skeleton (*28*, *29*). In contrast, mesonychids have comparatively generalized mammalian tarsals (*29*). Most cetaceans lack hind limbs, but recovery of reduced tarsal bones in middle-to-late Eocene archaeocetes *Dorudon* and *Basilosaurus* from Egypt (*30*) raised hope that earlier archaeocetes might retain tarsals that could be compared with artiodactyls and mesonychids.

Primitive archaeocetes are best known from shallow marine sedimentary rocks of early and middle Eocene age deposited in the eastern Tethys Sea in what is now India and Pakistan. In the year 2000, we found two partially articulated skeletons of early Protocetidae preserving fore- and hind limbs. Protocetidae are generally considered to be ancestral to later Basilosauridae and, hence, on the main line of cetacean evolution (*1*). One of the new skeletons represents a new genus and species, and the second represents a new species within an existing genus. Both come from transitional beds at the top of the Habib Rahi Formation and base of the Domanda Formation in Lakha Kach syncline near Rakhni, in the eastern part of Balochistan Province, Pakistan. Habib Rahi limestones represent the early Lutetian high sea stand in the Indus Basin, and the age of the transitional zone yielding the whales described here is about 47 million years ago (Ma) (*31*, *32*). For comparison on the same time scale, the ages of pakicetids *Himalayacetus* (*12*) and *Pakicetus* (*6*) are about 53.5 and 48 Ma, respectively; the age of ambulocetid *Ambulocetus* (*7*) is between 48 and 47 Ma; and the age of basilosaurids *Basilosaurus* and *Dorudon* in Egypt (*30*) is about 37 Ma.

Artiocetus clavis, new genus and species (*33*), includes a virtually complete skull (Fig. 1) that increases the range of cranial forms and feeding specializations known in early Protocetidae. *Artiocetus* is distinctive in that its external nares are positioned well forward on the dorsal surface like those of land mammals, it has a narrower frontal shield than that of other protocetids (relative to both the length of the cranium and breadth of the cranial base), and it has a wide cranial base relative to its skull length (*29*). *Artiocetus* is slightly older geologically (circa 0.5 million years) than other early protocetids (*8*, *34*), and its proportions are likely to be primitive for the family.

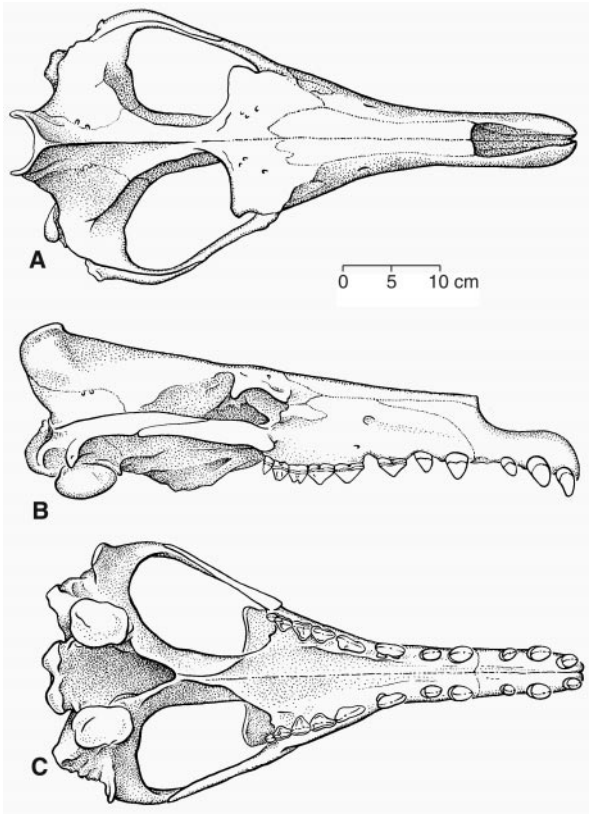

Fig. 1. Cranium of the holotype of *Artiocetus clavis*, GSP-UM 3458, new genus and species (**A** through **C**: dorsal, right lateral, and palatal views, respectively). Note anterior position of external nares, relatively narrow frontal shield, and broad cranial base of skull (*29*). Illustration: Bonnie Miljour.

The skeleton of *Artiocetus* was located after pieces of ankle bones, including a complete left astragalus, partial left calcaneum, and complete left cuboid, were found on the surface. Other bone pieces were traced upslope about 2 m to a point where a pelvis and lumbar vertebrae were lying in situ on a bedding plane. Excavation yielded the articulated thorax, cervical vertebrae, and, lastly, the skull (*29*). All are parts of the same specimen: no land mammals are known from this stratigraphic interval; no other mammalian specimens were found in the vicinity; all are similar in size, color, and preservation; and no parts are duplicated. The astragalus and cuboid (Fig. 2A) have characteristics that are clearly diagnostic of Artiodactyla. On the astragalus, the head has a well-developed navicular trochlea, the sustentacular facet is a proximodistally elongate oval on the ventral surface of the astragalus, and the ectal facet is a relatively small oval concavity on the lateral surface. The cuboid has the distinctive artiodactyl combination of a concave astragalar facet paired with a characteristically notched, convex, calcaneal facet.

Rodhocetus balochistanensis, new species (*35*), is referred to *Rodhocetus* because the new specimen has a femur with a relatively short, mediolaterally expanded shaft like that of the type species *R. kasrani* (*8*) (femoral shafts known for other early protocetids, including *Artiocetus*, are more cylindrical). The skull of *R. balochistanensis* is not well preserved. It was smaller but probably similar in proportions to that of *R. kasrani* (*29*). Axial skeletons of the two species can be compared, and that of *R. balochistanensis* is about 13% smaller in linear dimensions. Fore- and hind limbs are virtually complete and complement what was known of *Rodhocetus* previously. The wrist is that of a generalized mammal, broad and gently arched, with no carpal fusion and no centrale (Fig. 2B). Carpals are alternating rather than serial. The manus is mesaxonic, with the central digit (III) being longest and most robust. Proximal phalanges of digits II through IV were constrained to be habitually slightly extended by flat articular surfaces and large sesamoids on metacarpals II through IV. These are the digits with relatively short, broad, hoof-bearing distal phalanges (preserved in II and IV) (*29*). On land, *Rodhocetus* walked on a digitigrade hand, with the central digits II through IV bearing weight. Digit I is shorter than the others and more slender, whereas digit V is virtually the same length as II through IV and also slender. The lateral digits were not weight-bearing, but appear to have been retained to broaden a webbed hand.

Ankle bones of *Rodhocetus* (Fig. 2C) are long and narrow, with a deep tibial trochlea on

the astragalus constraining lateral mobility, and a substantial calcaneal tuber providing leverage for powerful foot extension. The astragalus and cuboid have the artiodactyl characteristics mentioned above, and, in addition, the calcaneum has the convex dorsal fibular facet characteristic of artiodactyls. The pes is paraxonic, with unusually long and thin metatarsals and phalanges (including terminal phalanges). Matching interosseous surfaces bordering the proximal halves of the metatarsal shafts show that these could be tightly compressed. Articulations both with the tarsus and with the phalanges indicate that the metatarsals were sometimes well separated. Contraction of intrinsic muscles narrowed the foot when it was tightly flexed. Unusual flanges of bone on the proximomedial base of middle phalanges II and III and on the proximolateral base of middle phalanges IV and V (arrows in Fig. 2C) provided leverage for opening the feet to maximum breadth during extension. Pedal phalanges cannot have been weight-bearing, but were elongated to stiffen a large webbed foot. On land *Rodhocetus* evidently walked on the plantar surface of the foot, with the calcaneum, plantar processes of other tarsals, and metatarsal sesamoids bearing weight, somewhat like eared seals do today. The structure of the hand is consistent with limited locomotion on land, but the foot shows that *Rodhocetus* was predominantly aquatic rather than terrestrial.

A skeletal restoration of *Rodhocetus* is shown in Fig. 3. Metapodials and phalanges of the hands and feet are similar to those described for *Ambulocetus natans* (*7*, *36*), but the hands of *Rodhocetus* are longer (about 165% of radius length in *Rodhocetus*, compared with 145% of radius length in *Ambulocetus*) and the feet are even longer (about 279% of radius length and 158% of femur length in *Rodhocetus*, compared with 197% of radius length and 121% of femur length in *Ambulocetus*). Thewissen and Fish (*37*) interpreted *Ambulocetus* as an otter-like pelvic paddler, and this is a good model for *Rodhocetus*. If the hands and feet were webbed as inferred here, then *Rodhocetus* was probably capable of quadrupedal paddling as well as pelvic paddling. The robust tail of *Rodhocetus* suggests that caudal undulation was important as well, especially while moving beneath the water surface. (Note that the length of the tail is not known.) The forelimbs and hands could not be extended as broad pectoral flippers, which would be required to control recoil from undulation or oscillation of a caudal fluke (*38*); hence, it is doubtful that *Rodhocetus* had such a fluke.

The previously known astragalus and cuboid of basilosaurid archaeocetes were too reduced and specialized to permit comparison with generalized land mammals (*30*). Inferences that astragali of Pakicetidae and Ambulocetidae are artiodactyl-like (*39*, *40*) have been questioned because the bones involved are fragmentary and not associated with diagnostic cetacean material (*13*). However, astragali and cuboids of *Artiocetus* and *Rodhocetus* described here are complete and in both cases were found with substantial protocetid skeletons (*29*). These indicate that cetaceans evolved from early artiodactyls, which corroborates results of many immunological, DNA hybridization, and molecular sequencing studies, and resolves a long-standing disagreement between paleontologists and molecular systematists. Although there is a general resemblance of the teeth of archaeocetes to those of mesonychids, such resemblance is sometimes overstated and evidently represents evolutionary convergence (*41*).

Close relationship of archaeocetes to artiodactyls casts new light on the morphology of primitive artiodactyls (*42*, *43*). *Rodhocetus* has a five-fingered mesaxonic hand, and the entocuneiform bears a facet for a first meta-

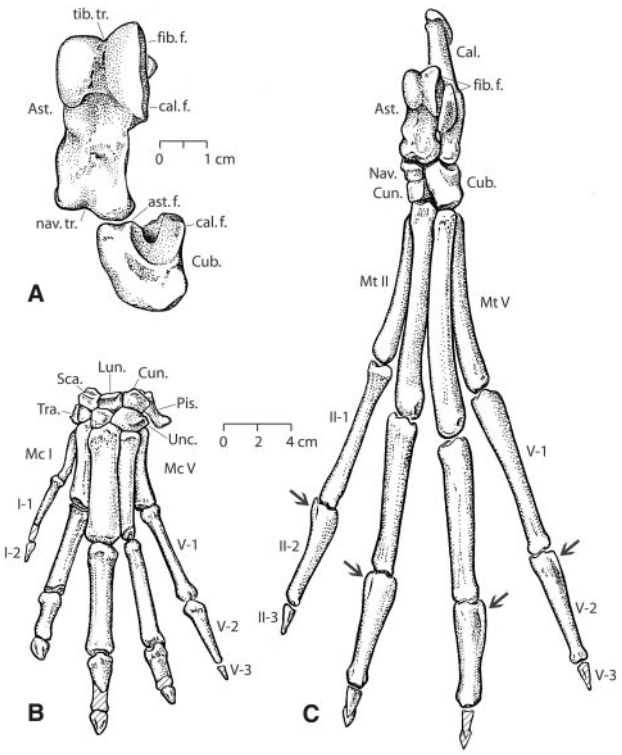

Fig. 2. Right astragalus and cuboid (**A**) of *Artiocetus clavis*, new genus and species, GSP-UM 3458, compared with virtually complete left manus (**B**) and left pes (**C**) of *Rodhocetus balochistanensis*, new species, GSP-UM 3485 (pes reversed from right side). All are shown in anterior view. Elements with oblique hatching were not recovered. Note artiodactyl characteristics in the well-developed navicular trochlea on the head of the astragalus, convex fibular facet on the calcaneum, and concave astragalar facet paired with a convex calcaneal facet notched into the cuboid. The hand is mesaxonic with three central weight-bearing toes that evidently bore nail-like hooves (distal phalanges preserved on digits II and IV) flanked by more gracile lateral toes that lacked hooves [distal phalanx preserved on digit I; see (*29*)]. The foot is paraxonic with four long toes, flanges of bone on the medial or lateral bases of the middle phalanges (arrows) providing leverage for opening the feet to maximum breadth during extension, and narrowly pointed ungules (distal phalanges preserved on digits II and III). Abbreviations: *Ast.*, astragalus; *ast. f.*, astragalar facet; *Cal.*, calcaneum; *cal. f.*, calcaneal facet; *Cub.*, cuboid; *Cun.*, cuneiform; *fib. f.*, fibular facet; *Lun.*, lunar; *Mc*, metacarpal; *Mt*, metatarsal; *Nav.*, navicular; *nav. tr.*, navicular trochlea; *Pis.*, pisiform; *Sca.*, scaphoid; *tib. tr.*, tibial trochlea; *Tra.*, trapezium; *Unc.*, unciform. Trapezoid and magnum are present in carpus but not separately labeled. Illustration: Bonnie Miljour.

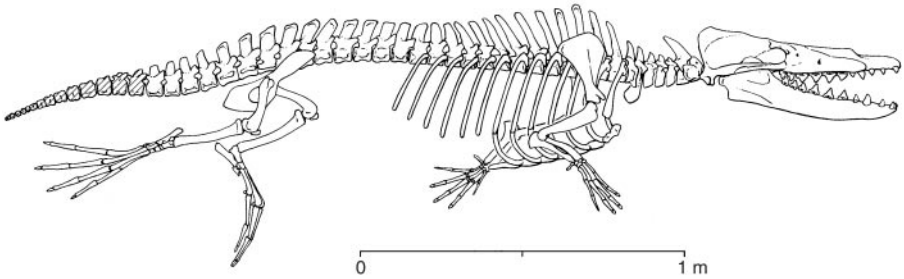

Fig. 3. Composite restoration of the skeleton of a paddling *Rodhocetus kasrani* (*8*) to show the morphology of this primitive protocetid. Limbs are scaled up 16% from *R. balochistanensis*, with the scapula restored from *A. clavis* and the proximal humerus restored from slightly later protocetids. Terminal vertebrae of the tail (hatched) are conjectural, and the tail was almost certainly longer than shown here. Forelimbs were probably folded against the body during rapid swimming by pelvic paddling at the sea surface and during rapid swimming by pelvic paddling and caudal undulation when submerged. On land, *Rodhocetus* supported itself on hoofed digits II, III, and IV of the hands and on the plantar surfaces of the feet, and probably progressed somewhat like a modern eared seal or sea lion. Illustration: Doug Boyer.

tarsal (Mt-I) retained from a formerly five-toed foot. These primitive characteristics are found in the oldest known artiodactyls like early Eocene *Diacodexis* (*42*, *44*), but also in later anthracotheriid artiodactyls such as late Eocene-Oligocene *Bothriodon* from Europe ("*Hyopotamus*") (*45*), and *Elomeryx* and possibly *Heptacodon* from North America (*46*, *47*). If hippopotamids are derived from anthracotheres (*48*), then it appears plausible that hippopotami may be the closest living relatives of whales.

References and Notes

1. R. E. Fordyce, L. G. Barnes, *Annu. Rev. Earth Planet. Sci.* **22**, 419 (1994).
2. G. G. Simpson, *Bull. Am. Mus. Nat. Hist.* **85**, 1 (1945).
3. A. Boyden, D. Gemeroy, *Zoologica* **35**, 145 (1950).
4. L. M. Van Valen, *Bull. Am. Mus. Nat. Hist.* **132**, 1 (1966).
5. F. S. Szalay, *Evolution* **23**, 703 (1969).
6. P. D. Gingerich, N. A. Wells, D. E. Russell, S. M. I. Shah, *Science* **220**, 403 (1983).
7. J. G. M. Thewissen, S. T. Hussain, M. Arif, *Science* **263**, 210 (1994).
8. P. D. Gingerich, S. M. Raza, M. Arif, M. Anwar, X. Zhou, *Nature* **368**, 844 (1994).
9. J. G. M. Thewissen, *J. Mammal. Evol.* **2**, 157 (1994).
10. M. C. McKenna, S. K. Bell, *Classification of Mammals Above the Species Level* (Columbia Univ. Press, New York, 1997), pp. 366–368.
11. W. P. Luckett, N. Hong, *J. Mammal. Evol.* **5**, 127 (1998).
12. S. Bajpai, P. D. Gingerich, *Proc. Natl. Acad. Sci. U.S.A.* **95**, 15464 (1998).
13. M. A. O'Leary, J. H. Geisler, *Syst. Biol.* **49**, 455 (1999).
14. Z. Luo, P. D. Gingerich, *Univ. Mich. Pap. Paleontol.* **31**, 1 (1999).
15. D. Graur, D. G. Higgins, *Mol. Biol. Evol.* **11**, 357 (1994).
16. C. Montgelard, F. M. Catzeflis, E. Douzery, *Mol. Biol. Evol.* **14**, 550 (1997).
17. F. G. R. Liu, M. M. Miyamoto, *Syst. Biol.* **48**, 54 (1999).
18. J. K. Lum *et al.*, *Mol. Biol. Evol.* **17**, 1417 (2000).
19. V. M. Sarich, in *Mammal Phylogeny: Placentals*, F. S. Szalay, M. J. Novacek, M. C. McKenna, Eds. (Springer, New York, 1993), pp. 103–114.
20. D. M. Irwin, U. Arnason, *J. Mammal. Evol.* **2**, 37 (1994).
21. J. E. Gatesy, C. Hayashi, M. A. Cronin, P. Arctander, *Mol. Biol. Evol.* **13**, 954 (1996).
22. M. Shimamura *et al.*, *Nature* **388**, 666 (1997).
23. B. Ursing, U. Arnason, *Proc. R. Soc. London Ser. B* **265**, 2251 (1998).
24. M. Nikaido, A. P. Rooney, N. Okada, *Proc. Natl. Acad. Sci. U.S.A.* **96**, 10261 (1999).
25. J. E. Gatesy, M. C. Milinkovitch, V. G. Waddell, M. J. Stanhope, *Syst. Biol.* **48**, 6 (1999).
26. R. G. Kleineidam, G. Pesole, H. J. Breukelman, J. J. Beintema, R. A. Kastelein, *J. Mol. Evol.* **48**, 360 (1999).
27. U. Arnason, A. Gullberg, S. Gretarsdottir, B. Ursing, A. Janke, *J. Mol. Evol.* **50**, 569 (2000).
28. B. Schaeffer, *Am. Mus. Novit.* **1356**, 1 (1947).
29. Web figs. 1 through 7, Web table 1, and supplemental text are available at *Science* Online at www.sciencemag.org/cgi/content/full/293/5538/2239/DC1.
30. P. D. Gingerich, B. H. Smith, E. L. Simons, *Science* **249**, 154 (1990).
31. W. A. Berggren, D. V. Kent, C. C. Swisher, M.-P. Aubry, in *Geochronology, Time Scales and Global Stratigraphic Correlations: A Unified Temporal Framework for an Historical Geology*, W. A. Berggren, D. V. Kent, M.-P. Aubry, J. A. Hardenbol, Eds. (Society of Economic Paleontologists and Mineralogists, Tulsa, 1995), special vol. 54, pp. 129–212.
32. J. A. Hardenbol *et al.*, in *Mesozoic and Cenozoic Sequence Stratigraphy of European Basins*, P.-C. d. Graciansky, J. A. Hardenbol, T. Jacquin, P. R. Vail, Eds. (SEPM Society for Sedimentary Geology, Special Publication 60, 1998), pp. 3–13 (eight charts).
33. Order Cetacea, Suborder Archaeoceti, Family Protocetidae. *Artiocetus clavis*, new genus and species. **Etymology**: *artios*, entire or even-numbered, and *ketos*, Gr., whale; *clavis*, L., key or clavicle; reflecting possession of shared characteristics of Artiodactyla and Cetacea, and alluding to both the key intermediacy of this taxon and retention of a rudimentary clavicle in the shoulder girdle. **Holotype**: GSP-UM 3458 (Geological Survey of Pakistan–University of Michigan collection, Quetta): virtually complete skull with much of the axial skeleton; parts of the shoulder girdle and forelimb including a rudimentary clavicle, scapula, distal radius and ulna; and parts of pelvic girdle and hind limb including an ilium, distal femur with a patella, and complete astragalus and cuboid. Eruption of all permanent teeth and fusion of most epiphyses shows that the specimen was fully mature. **Type locality**: Kunvit, Kohlu District, eastern Balochistan Province, Pakistan (30°05′44′N latitude, 69°47′20″E longitude). **Diagnosis**: Medium-sized protocetid archaeocete (estimated weight, 420 kg) with a skull distinctive in having anteriorly positioned nares, a relatively narrow frontal shield, and a relatively broad cranial base (*29*). Femoral shaft is roughly cylindrical. Astragalus differs from that in contemporary *Rodhocetus balochistanensis* in being smaller and relatively lower, with smaller ectal and fibular facets. **Description**: See supplementary material (*29*).
34. P. D. Gingerich, M. Arif, W. C. Clyde, *Contrib. Mus. Paleont. Univ. Mich.* **29**, 291 (1995).
35. Order Cetacea, Suborder Archaeoceti, Family Protocetidae. Genus *Rodhocetus* Gingerich *et al.* (*8*). *Rodhocetus balochistanensis*, new species. **Etymology**: *balochistanensis*, referring to provenence of type specimen. **Holotype**: GSP-UM 3485: braincase of skull with much of axial skeleton; parts of forelimb including distal humerus, radius and ulna, virtually complete carpus and manus; and parts of pelvic girdle and hind limb including acetabular rim of pelvis, femur, patellae, tibia, virtually complete tarsus and pes. Fusion of most epiphyses shows that the specimen was fully mature. **Type locality**: Kunvit, Kohlu District, eastern Balochistan Province, Pakistan (30°05′20″N latitude, 69°47′39″E longitude). **Diagnosis**: Smaller *Rodhocetus* [estimated body weight, 450 kg compared with 590 kg in *R. kasrani*; see (*49*)]. Anterior thoracic vertebrae average 13% smaller in linear dimensions (meaning *R. kasrani* is 16% larger), whereas the femur is slightly longer. Femoral shaft has a more distinct third trochanter but is otherwise similarly diamond-shaped in cross-section. Astragalus differs from that in contemporary *Artiocetus clavis* in being larger and relatively higher, with larger ectal and fibular facets. **Description**: See supplementary material (*29*).
36. J. G. M. Thewissen, S. I. Madar, S. T. Hussain, *Cour. Forschungsinst. Senckenb. Frankfurt* **191**, 1 (1996).
37. J. G. M. Thewissen, F. E. Fish, *Paleobiology* **23**, 482 (1997).
38. P. W. Webb, *Am. Zool.* **28**, 709 (1988).
39. J. G. M. Thewissen, S. I. Madar, S. T. Hussain, *Nature* **395**, 452 (1998).
40. J. G. M. Thewissen, S. I. Madar, *Syst. Biol.* **48**, 21 (1999).
41. G. J. P. Naylor, D. C. Adams, *Syst. Biol.* **50**, 444 (2001).
42. K. D. Rose, *Science* **216**, 621 (1982).
43. K. D. Rose, *Proc. Natl. Acad. Sci. U.S.A.* **93**, 1705 (1996).
44. J. G. M. Thewissen, S. T. Hussain, *Anat. Histol. Embryol. Zentralbl. Veterinarmed. C* **19**, 37 (1990).
45. W. Kowalevsky, *Philos. Trans. R. Soc. London* **163**, 19 (1873).
46. W. B. Scott, *J. Acad. Nat. Sci. Philadelphia* **9**, 461 (1894).
47. W. B. Scott, *Trans. Am. Philos. Soc.* **28**, 363 (1940).
48. E. H. Colbert, *Am. Mus. Novit.* **799**, 1 (1935).
49. P. D. Gingerich, in *The Emergence of Whales: Evolutionary Patterns in the Origin of Cetacea*, J. G. M. Thewissen, Ed. (Plenum, New York, 1998), pp. 423–449.

50. We thank Hasan Ghaur, A. Latif Khan, S. Ghazanfar Abbas, and Imran Khan, Geological Survey of Pakistan, Quetta, for encouragement and logistical support in the field. Specimens were prepared by W. J. Sanders, J. Groenke, and D. Erickson at the University of Michigan. P. Myers provided access to comparative collections of mammals in the University of Michigan Museum of Zoology and J. G. M. Thewissen provided casts of previously described astragali. W. C. Clyde, D. C. Fisher, R. E. Fordyce, K. D. Rose, W. J. Sanders, B. H. Smith, J. G. M. Thewissen, and M. D. Uhen read and improved the manuscript. Field and laboratory research was supported by NGS (5072-93) and NSF (EAR-9714923).

28 June 2001; accepted 15 August 2001

Rapid Diversification of a Species-Rich Genus of Neotropical Rain Forest Trees

James E. Richardson,[1,2] R. Toby Pennington,[1]* Terence D. Pennington,[3] Peter M. Hollingsworth[1]

Species richness in the tropics has been attributed to the gradual accumulation of species over a long geological period in stable equatorial climates or, conversely, to speciation in response to late Tertiary geological events and unstable Pleistocene climates. DNA sequence data are consistent with recent diversification in *Inga*, a species-rich neotropical tree genus. We estimate that speciation was concentrated in the past 10 million years, with many species arising as recently as 2 million years ago. This coincides with the more recent major uplifts of the Andes, the bridging of the Isthmus of Panama, and Quaternary glacial cycles. *Inga* may be representative of other species-rich neotropical genera with rapid growth and reproduction, which contribute substantially to species numbers in the world's most diverse flora.

The neotropical flora comprises about 90,000 plant species—37% of the world's total and more than the floras of tropical Africa (35,000 spp.) and Asia (40,000 spp.) combined (*1*). Most of these species are found in rain forests, which have higher plant species diversity than any other habitat on the planet. How this diversity arose is unexplained (*2*, *3*). Early theories (the "museum model") suggested that a stable tropical climate allowed species to accumulate over time, with low rates of extinction in the absence of major environmental perturbations